The plasmonic resonant absorption in GaN double-channel high electron mobility transistors

Lin Wang, Xiao-Shuang Chen,[a] Wei-Da Hu,[a] Jun Wang, Jian Wang, Xiao-Dong Wang, and Wei Lu

National Laboratory for Infrared Physics, Shanghai Institute of Technical Physics, Chinese Academy of Sciences, Shanghai 200083, China

(Received 21 April 2011; accepted 10 July 2011; published online 8 August 2011)

We have investigated the plasmonic oscillations in GaN double-channel (DC) high electron mobility transistors (HEMTs). It is shown that the absorption peaks of DC-HEMT can exist in wider frequency regions than that of single channel HEMT. These absorption peaks appear as a result of excitation of elementary plasmon modes supported by separate channels and can be tuned for the entire terahertz domain. Significant resonant enhancement is also observed after varying the two-dimensional electron gas density in DC-HEMTs. These promising properties indicate that DC-HEMTs can have important applications as voltage tunable broadband terahertz detectors, intensity modulators, and filters. © *2011 American Institute of Physics*. [doi:10.1063/1.3619842]

Since the last decade, terahertz (THz) spectroscopy, imaging systems, and techniques have attracted extensive attention[1,2] for various applications, such as explosive and weapon detection, pharmaceutical quality control, biomedical applications, and nondestructive evaluation/quality control. These applications require THz detectors with fast response times. The most common THz detectors available now include bolometers,[3] pyroelectric detectors, and schottky diodes.[4] Recently, there has been growing interest in so-called plasma wave field effect transistors.[5–9] A two-dimensional electron gas (2DEG) is utilized to obtain the plasmonic resonant oscillations in the THz range.[10–15]

For GaAs HEMTs, the resonant condition is satisfied after scaling the length of gate fingers into submicron region[16,17,19–21]. While Muravjov *et al.*[13] indicate that large-area slit-grating-gate AlGaN/GaN-based HEMTs possess wide tunability of resonances as a function of gate voltage due to high electron density induced by a strong polarization effect. However, the plasmonic resonant properties in GaN-based double channel (DC) HEMTs have not yet been reported despite success in the recent fabrication of such devices [22,23]. In this letter, we mainly focus on the plasmonic resonances in DC-HEMTs. It is shown that wide resonant frequency regions can be obtained.

A DC-HEMT structure with 0.7-duty-cycle grating gate (0.6 μm period) is shown in Fig. 1 schematically. Due to the strong polarization effect of nitride semiconductors, 2DEG channels around 30 nm thick can be well confined at AlGaN/GaN heterointerfaces.[22] Further capacitance–voltage (CV) profiling results indicate that the electron densities of upper (N_U) and lower (N_L) channels are about 7×10^{18} cm^{-3} and 3×10^{18} cm^{-3} under zero gate voltage. In this letter, the plasmonic oscillations in DC-HEMT are simulated by using a finite difference scheme, and the Drude conductivity[24,25] is modeled by a recursive convolution method to describe the electromagnetic wave motions along the channel.

The resonant absorption spectra of DC-HEMT (solid line) and AlGaN/GaN single channel (SC) HEMT (dashed line) are shown in Fig. 2(a) for comparison purposes. Due to the plasmonic oscillation induced in the lower channel, a small blue shift and enhancement of the second resonant peak are displayed in the spectrum of DC-HEMT (the electron density in SC-HEMT is also 7×10^{18} cm^{-3}). However, no splitting of resonant peak takes place in the spectrum of DC structure as compared with that of SC structure. These phenomena will be explained below.

For clarity, the dipole distributions of resonant plasmonic peaks along the channel of SC-HEMT are extracted and shown in the inset of Fig. 2(a) (plus/minus sign represents depletion/accumulation of electrons). Two kinds of elementary plasmon modes with charge distribution symmetry and asymmetry along the channel can be found. In this letter,

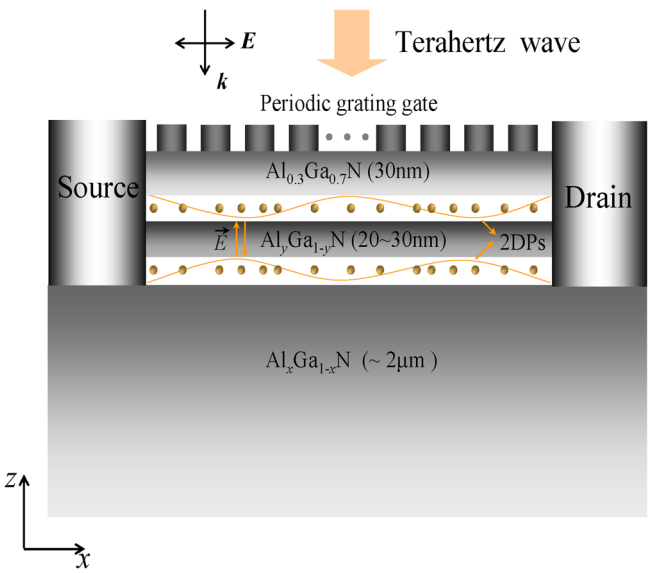

FIG. 1. (Color online) Sketch of DC-HEMTs' structure. The terahertz wave is incident from the top with a linear polarization electric field E, wave vector k. The inter-channel electric field E and current density vibrations along the two channels are also shown schematically.

[a]Authors to whom correspondence should be addressed. Electronic address: xschen@mail.sitp.ac.cn and wdhu@mail.sitp.ac.cn.

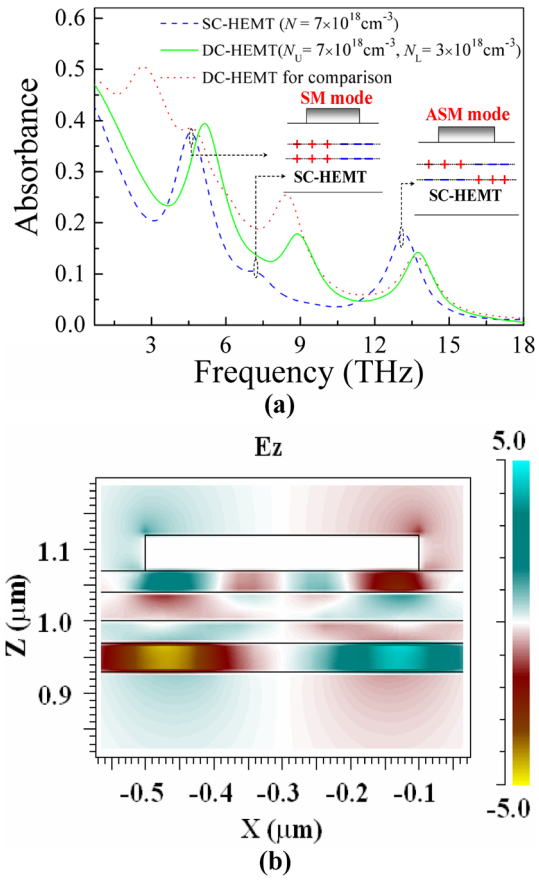

FIG. 2. (Color online) (a) THz absorption spectra of SC-HEMT (dashed line) and DC-HEMT (solid line). The dipole distributions along the channel of SC-HEMT are shown in the inset. The absorption spectrum of DC-HEMT with 10nm thick barrier and 5nm inter-channel separation is shown in dotted line. (b) The plasmon-induced electric field distribution in DC-HEMT

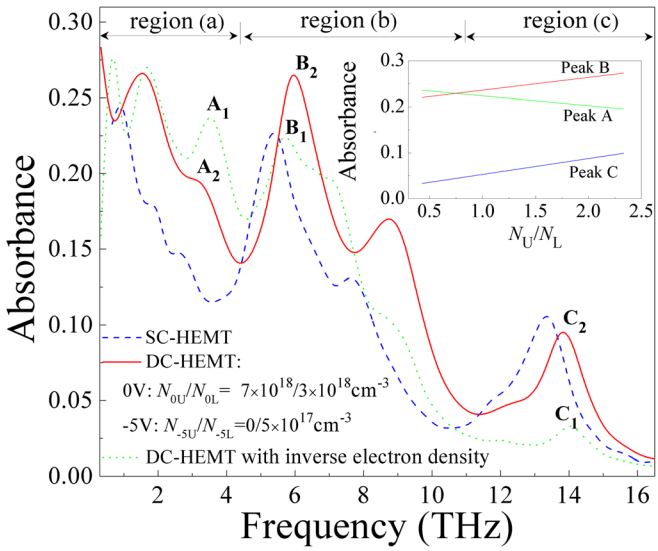

FIG. 3. (Color online) The absorption spectra of DC and SC HEMTs (dashed line) with periodic gate voltages. The solid line is the spectrum of DC-HEMT with 0/-5V periodic voltages. The dotted line is the spectrum of DC-HEMT with density distributions under zero gate voltage inverted. Additionally, the relative variations of heights of resonant peaks A(A_1, A_2), B(B_1, B_2), and C(C_1, C_2) are shown in the inset as a function of the ratio between electron densities of upper and lower channels under one electrode, the voltage of adjacent electrode is -5V.

we call these two plasmon modes "SM" (symmetrical plasmon mode) and "ASM" (asymmetrical plasmon mode) modes. Since the model proposed by Dyakonov and Shur in Ref. 15 is one-dimensional and the plasma waves mainly transport along the x direction, the Dyakonov–Shur waves are mostly relevant to the SM modes. The first two resonant peaks follow the simple linear dispersion relation, $\omega = sk$ with the wave vector $(n + 1/2)\pi/l_{eff}$, in which l_{eff} is the effective gate length and where the values of the mode index n are 1 and 2, respectively. The ASM mode has not yet been indicated in previous work. But recently, a plasmon mode similar to ASM mode is found in 2DEG shells in Ref. 26.

It is known that the plasmon response of complex nanostructures can be viewed as the interaction and/or hybridization of elementary plasmons supported by nanostructures of elementary geometries.[27] The electromagnetic interaction between these "free" plasmons leads to mixing, splitting, and shifts of the plasmonic resonances. In our case, the plasmon response of DC system can also be viewed as an electromagnetic interaction between elementary plasmons supported by separate channels. For a better visualization, the plasmon-induced electric field distribution at 9THz (solid line in Fig. 2(a)). It can be seen that this peak is related to plasmon mixing mode caused by the interaction between ASM (lower channel) and SM (upper channel) plasmons.

If the thickness of the barrier layer and the separation between the two channels are reduced, splitting of the SM mode takes place at around 3 THz (see dotted line in Fig. 2(a)). The strength of the resonant peak at 9 THz is also significantly enhanced. These effects occur because interactions between plasmons in the two channels are enhanced. However, no splitting of the ASM mode occurs in this situation. Our calculations indicate that the splitting of ASM mode is related to the electron density distributions in the two channels. This effect can be observed until the plasmons of ASM mode in the two channels are near resonant with each other through modulating the gate voltage.

Now we can turn our attention to the THz absorption properties in the case of periodic electron density distributions by applying periodic voltages. The absorption spectra of DC-HEMT and SC-HEMT are shown in Fig. 3 for comparison. The spectra can be divided into three distinguishable frequency domains, (a) plasmonic resonances in the region 0.5 ~ 4THz with low electron density, (b) plasmonic resonance in the region 4 ~ 11THz with high electron density, and (c) plasmonic resonance in the region 11 ~ 16THz. Stronger resonant peaks of DC-HEMT compared with SC HEMT are clearly visible in region (a). In DC-HEMT, enhanced resonant absorptions can also be found in this region (dotted line) since the absorbance of peak A increases by 20% (after comparing peaks A_1 and A_2). This result can be achieved by applying negative voltage for devices with good buffer isolation as in Ref. 28. In region (b), the strength of resonant peaks is also stronger for DC-HEMT, which is similar to above-mentioned situation as in Fig. 2(a). Hence it is indicated that stronger plasmonic resonances can be found in mixing plasmon modes.

In the inset of Fig. 3, the variations in strength of different resonant peaks are shown as a function of the ratio between electron densities of the upper and lower channels. It can be seen that the absorbance of peak A decreases after

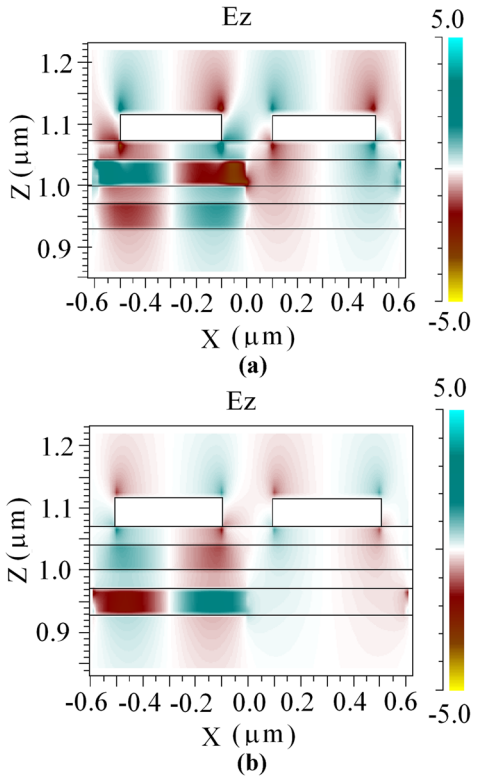

FIG. 4. (Color online) Schematic of plasmon-induced electric field distributions under gate electrodes: (a) plasmonic oscillation corresponding to peak C_2 in Fig. 3 and (b) plasmonic oscillation corresponding to peak C_1 in Fig. 3. The channels with higher electron density are shown at left half of these figures.

increasing the ratio, while the absorbance of peaks B and C increases. According to the plasma wave dispersion law, the wave vector of a plasma wave is smaller in the region with higher electron density. The plasmonic oscillation in region (c) is dominated by the oscillation of the ASM mode along the channel with higher electron density (see next paragraph). Therefore, the plasmonic oscillations in regions (b) and (c) are mainly confined to the locations in the channels with high electron density. As for plasmonic oscillations in region (a), leakage of plasmonic energy into adjacent channels can take place. In view of this, the variation of the strength of peak A in the inset of Fig. 3 is mainly caused by the effect of adjacent channels, while the variations of peaks B and C may be related to the polarization-field effect of the electrodes.

Plasmon-induced electric field distributions (peaks C_1 and C_2 in Fig. 3) are shown in Fig. 4. It can be seen that stronger plasmonic oscillation occurs when the ratio between electron densities of the upper and lower channels is 7:3. The plasmons of these two peaks are mainly related to the oscillations along the channel of higher electron density since there are no significant field discontinuities in the channel of lower density. Also, there is no indication of significant plasmonic oscillations in Fig. 4(b) due to the weakness of polarization field.

In conclusion, we have indicated that more absorption peaks can be realized in DC-HEMT as a result of interaction between elementary plasmons supported by separate channels. These absorption peaks can be tuned in frequency throughout the entire terahertz domain by changing the distributions of electron density in the channels. Additionally, resonance enhancement can be observed at certain frequencies after applying appropriate gate voltages. Further improvement of the resonant properties will rely on appropriate design of grating-gate couplers and optimization of device structures.

The work was supported by the State Key Program for Basic Research of China (2007CB613206, 2011CB22004), National Natural Science Foundation of China (61006090, 10725418, 10734090, 10990104, 60976092), Fund of Shanghai Science and Technology Foundation (09DJ1400203, 09dz2202200, 10JC1416100, 10510704700).

[1]N. Pala and M. S. Shur, Electron. Lett. **44**, 1391 (2008)
[2]A. Redo-Sanchez and X. C. Zhang, IEEE J. Sel. Top. Quantum Electron. **14**, 260 (2008).
[3]M. Kroug *et al.*, IEEE Trans. Appl. Supercond. **11**, 962 (2001).
[4]S. Barbieri *et al.*, Opt. Lett. **29**, 1632 (2004).
[5]M. S. Shur and J.-Q. Lü, IEEE Trans. Microwave Theory Tech. **48**, 750 (2000).
[6]D. Veksler *et al.*, Phys. Rev. B **73**, 125328 (2006).
[7]M. Dyakonov and M. S. Shur, Appl. Phys. Lett. **87**, 111501 (2005).
[8]W. Knap *et al.*, Appl. Phys. Lett. **81**, 4637 (2002).
[9]T. A. Elkhatib *et al.*, IEEE Trans. Microwave Theory Tech. **58**, 331 (2010).
[10]A. EI Fatimy *et al.*, J. Appl. Phys. **107**, 024504 (2010).
[11]T. Ostuji *et al.*, J. Phys.: Condens. Matter. **20**, 384206 (2008).
[12]D. Coquillat *et al.*, Opt. Express **18**, 6024 (2010).
[13]A. V. Muravjov *et al.*, Appl. Phys. Lett. **96**, 042105 (2010).
[14]M. Dyakonov and M. S. Shur, IEEE Trans. Electron Devices **43**, 380 (1996).
[15]M. Dyakonov and M. S. Shur, Phys. Rev. Lett. **71**, 2465 (1993).
[16]M. Dyakonov and M. S. Shur, IEEE Trans. Electron Devices **43**, 1640 (1996).
[17]T. Otsuji *et al.*, J. Phys: Condens. Matter. **20**, 1 (2008).
[18]V. V. Popov, G. M. Tsymbalov, and M. S. Shur, J. Phys: Condens. Matter. **20**, 1 (2008).
[19]A. EI. Fatimy *et al.*, Appl. Phys. Lett. **89**, 131926 (2006).
[20]F. Teppe *et al.*, Appl. Phys. Lett. **89**, 222109 (2006).
[21]O. Ambacher *et al.*, J. Phys.: Condens. Matter. **14**, 3399 (2002).
[22]R. M. Chu *et al.*, IEEE Trans. Electron Devices **52**, 438 (2005).
[23]S. Zhang *et al.*, Appl. Phys. Lett. **95**, 212101 (2009).
[24]V. V. Popov *et al.*, Appl. Phys. Lett. **93**, 263503 (2008).
[25]D. S. Kainth, D. Richards, A. S. Bhatti, H. P. Hughes, M. Y. Simmons, E. H. Linfield, and D. A. Ritchie, Phys. Rev. B **59**, 2095 (1999).
[26]T. V. Teperik *et al.*, Appl. Phys. Lett. **90**, 251910 (2007).
[27]E. Prodan *et al.*, Science **302**, 419 (2003).
[28]Z. Chen *et al.*, Appl. Phys. Lett. **94**, 171117 (2009).